Epithelial Membrane Protein 2 Governs Transepithelial Migration of Neutrophils into the Airspace

Wan-Chi Lin*, Kymberly M. Gowdy*, Jennifer H. Madenspacher, Rachel L. Zemans, Kazuko Yamamoto, Miranda Lyons-Cohen, Hideki Nakano, Kyathanahalli Janardhan, Carmen J. Williams, Donald N. Cook, Joseph P. Mizgerd, Michael B. Fessler

*These authors contributed equally.

SUPPLEMENTAL INFORMATION

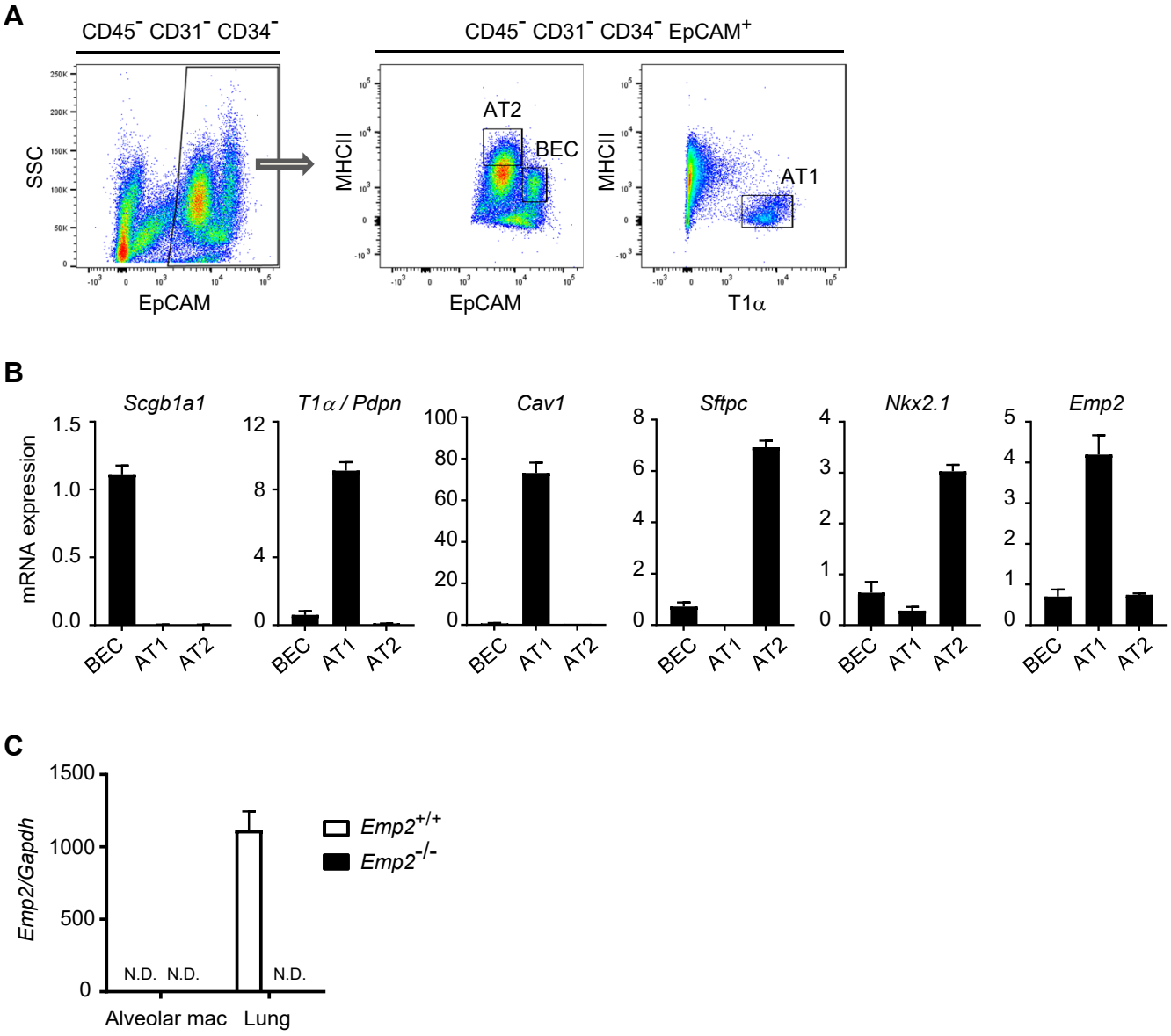

Supplemental Figure 1. EMP2 expression and alveolar epithelial cell gating by flow cytometry. (**A**) Epithelial cell fluorescence-activated cell sorting strategy is shown. Lungs from wild type mice were digested for analysis. Lineage ($CD45^{-}CD31^{-}CD34^{-}$)-negative, 7AAD-negative cells were evaluated for MHCII, EpCAM, and T1α. $EpCAM^{+}$ cells that were $MHCII^{+}/EpCAM^{int}$ (AT2 cells), $MHCII^{-}/EpCAM^{hi}$ (bronchiolar epithelial cells [BEC]), and $T1\alpha^{+}$ (AT1 cells) were collected by fluorescence-activated cell sorting. (**B**) RT-qPCR was conducted for secretoglobin family 1A member 1 (*Scgb1a1;* a BEC marker), T1α/Podoplanin (*Pdpn)* and *Cav1* (AT1 markers), surfactant protein C *(Sftpc;* an AT2 marker), NK2 Homeobox 1 (*Nkx2.1;* AT2 marker, also expressed by Club cells in BEC), as well as *Emp2*, as shown. (**C**) RT-qPCR for *Emp2* mRNA was performed on alveolar macrophages collected by BAL and on non-lavaged lung tissue from naïve $Emp2^{+/+}$ and $Emp2^{-/-}$ mice. N.D.= not detected. Data are the mean ± SEM and are representative of at least 3 independent experiments.

Supplemental Figure 2

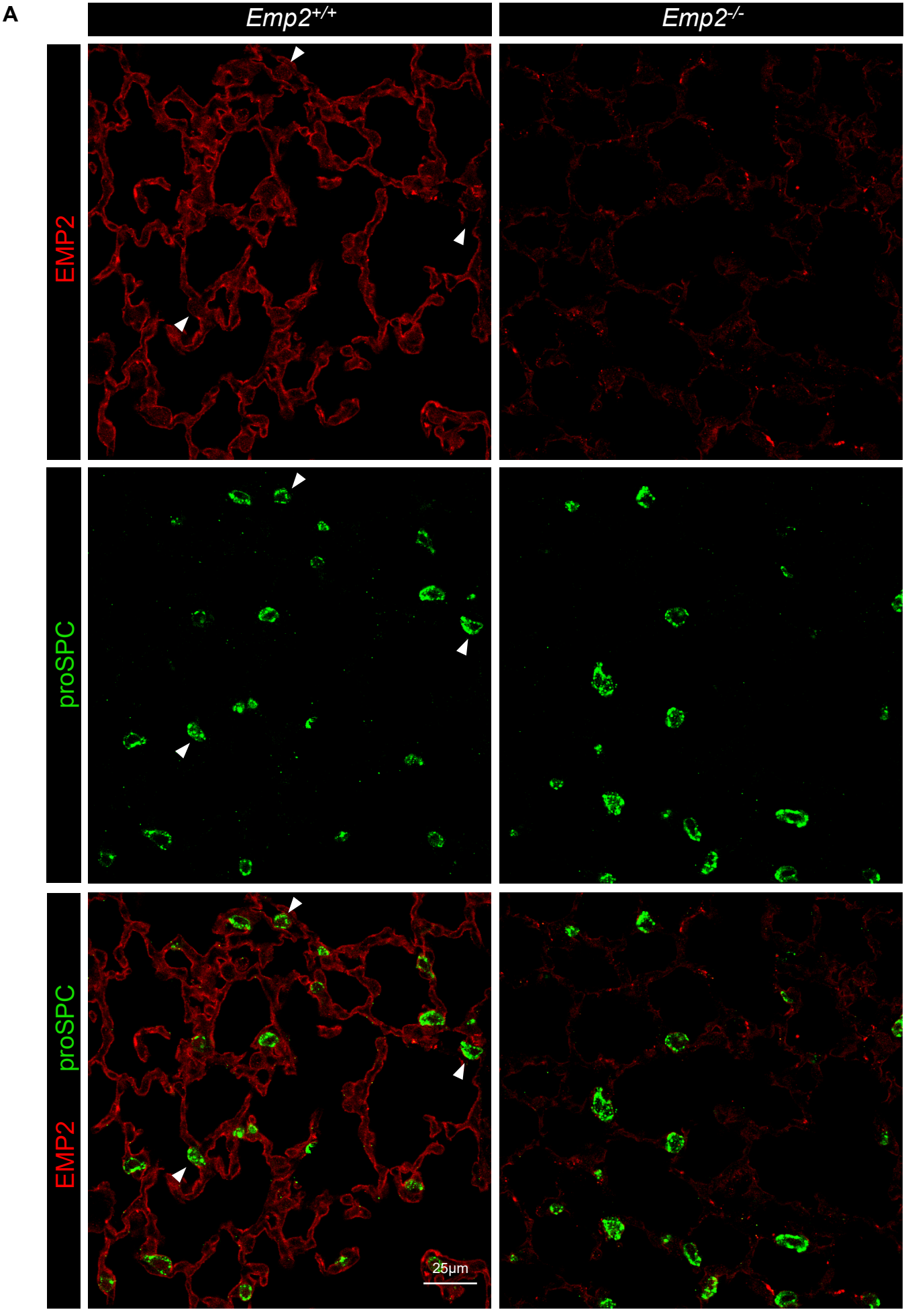

B

c

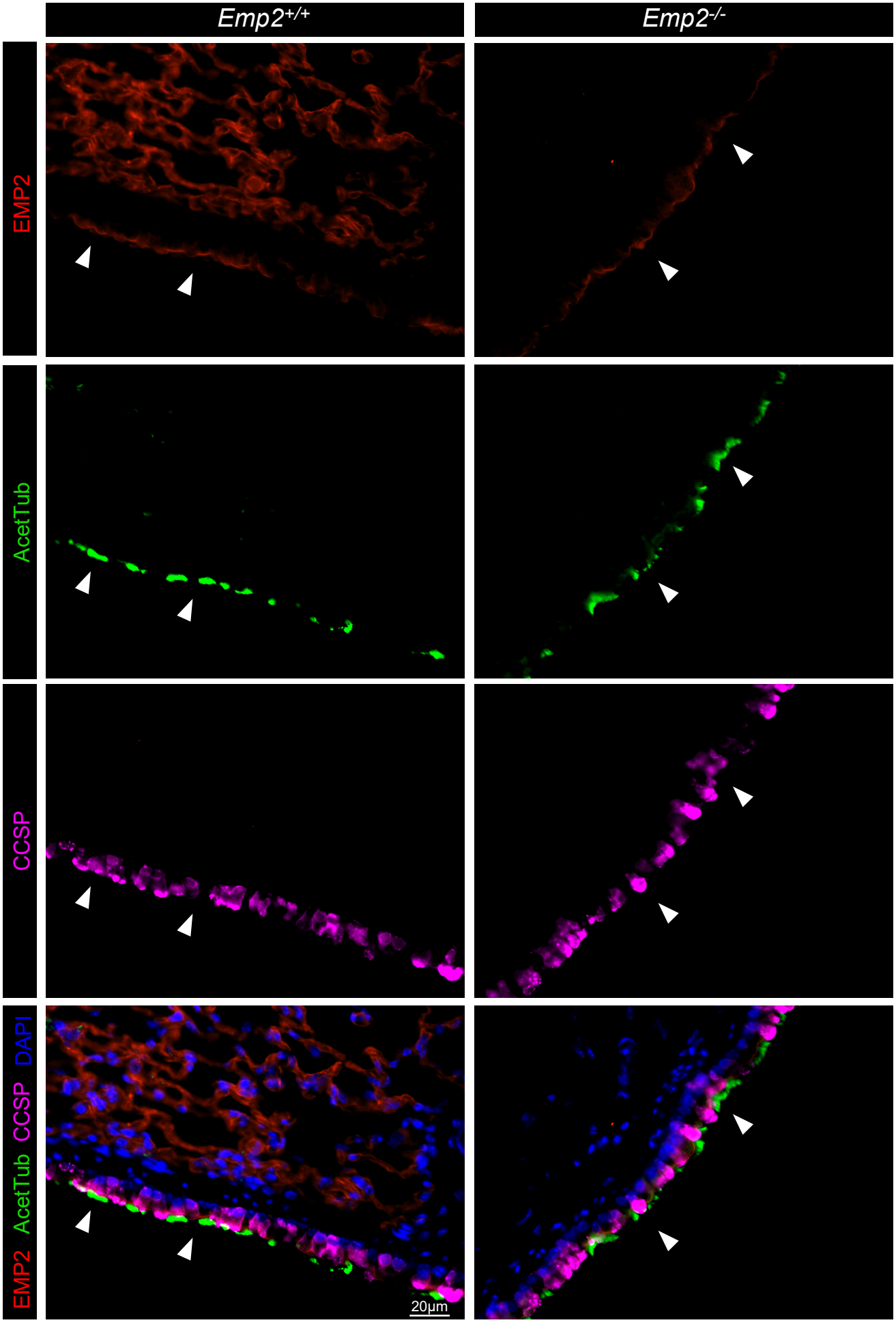

Supplemental Figure 2. EMP2 is expressed in AT1 but not AT2, Club, or ciliated cells. (**A**) Lung sections from *Emp2*$^{+/+}$ and *Emp2*$^{-/-}$ mice were immunostained for EMP2 and surfactant protein C (SPC). Arrowheads indicate ATII cells. (**B**) Lung sections from *SftpcCreERT2*$^{+/-}$;*Rosa26-mTmG*$^{+/-}$ mice were stained for EMP2, GFP, and T1α. Open arrowheads indicate AT1 cells. Closed arrowheads indicate points at which AT2 cells comprise the apical epithelial surface, as indicated by expression of GFP with gaps in T1α and EMP2 staining. (**C**) Lung sections from *Emp2*$^{+/+}$ and *Emp2*$^{-/-}$ mice were immunostained for EMP2, Club cell secretory protein (CCSP, a Club cell marker), and acetylated tubulin (a ciliated cell marker). Arrowheads indicate nonspecific staining with the EMP2 antibody, which is seen in both *Emp2*$^{+/+}$ and *Emp2*$^{-/-}$ mice airways. Images were taken at 40-63x magnification and are representative of n≥3 mice.

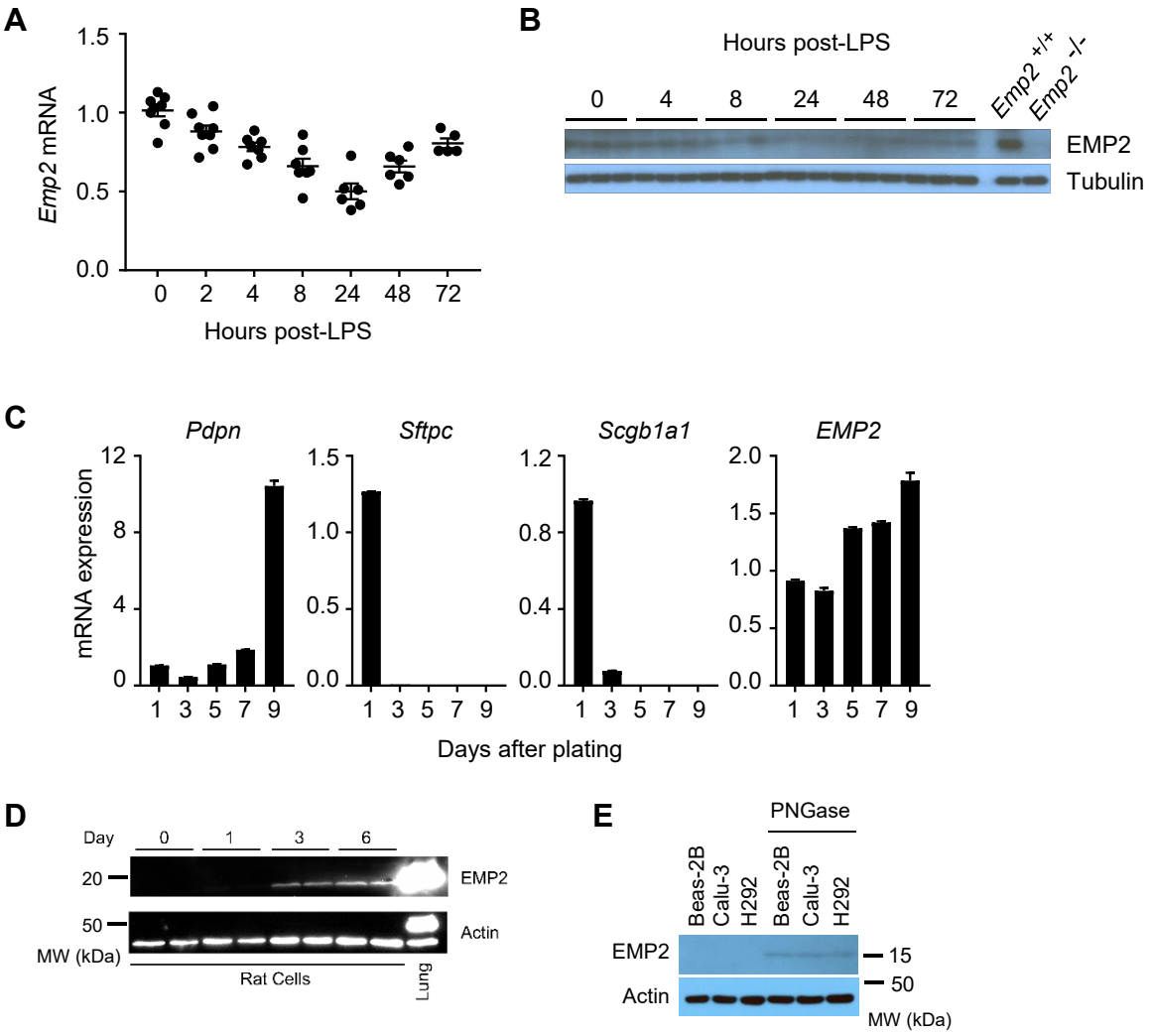

Supplemental Figure 3. Expression of EMP2 protein in lung tissues and epithelial cells. (**A-B**) C57BL/6 mice were exposed to aerosolized LPS (300 μg/ml x 30 min). At various time points post-exposure, lung homogenates were analyzed by RT-qPCR for *Emp2* mRNA (A), or by immunoblot for EMP2 and tubulin (loading control) protein (B). In the immunoblot, replicate mice are shown for each time point, and *Emp2*$^{-/-}$ mouse lung is shown as a control. (**C**) Epithelial cells were purified from WT mouse lung and then cultured for 14 days to induce an AT1-like cell phenotype. On the culture days shown, podoplanin (*Pdpn*; AT1 marker), surfactant protein C (*Sftpc*, an AT2 marker), secretoglobin family 1A member 1 (*Scgb1a1;* bronchiolar epithelial cell marker), and *Emp2* mRNA were quantified by RT-qPCR (mean ± SEM). (**D**) Rat lung AT2 cells were purified and cultured *ex vivo* over a time course as shown (duplicate wells). At the various durations of culture shown, EMP2 was immunoblotted in cell lysates. Murine *Emp2*$^{+/+}$ lung homogenate is shown as a control. Molecular weight is marked at left. (**E**) Cell lysates from Beas-2B, Calu-3, and H292 cells were immunoblotted for EMP2 and actin (loading control) before and after treatment with PNGase to remove glycosylation, yielding EMP2 at its expected molecular weight. Data are representative of at least 3 independent experiments.

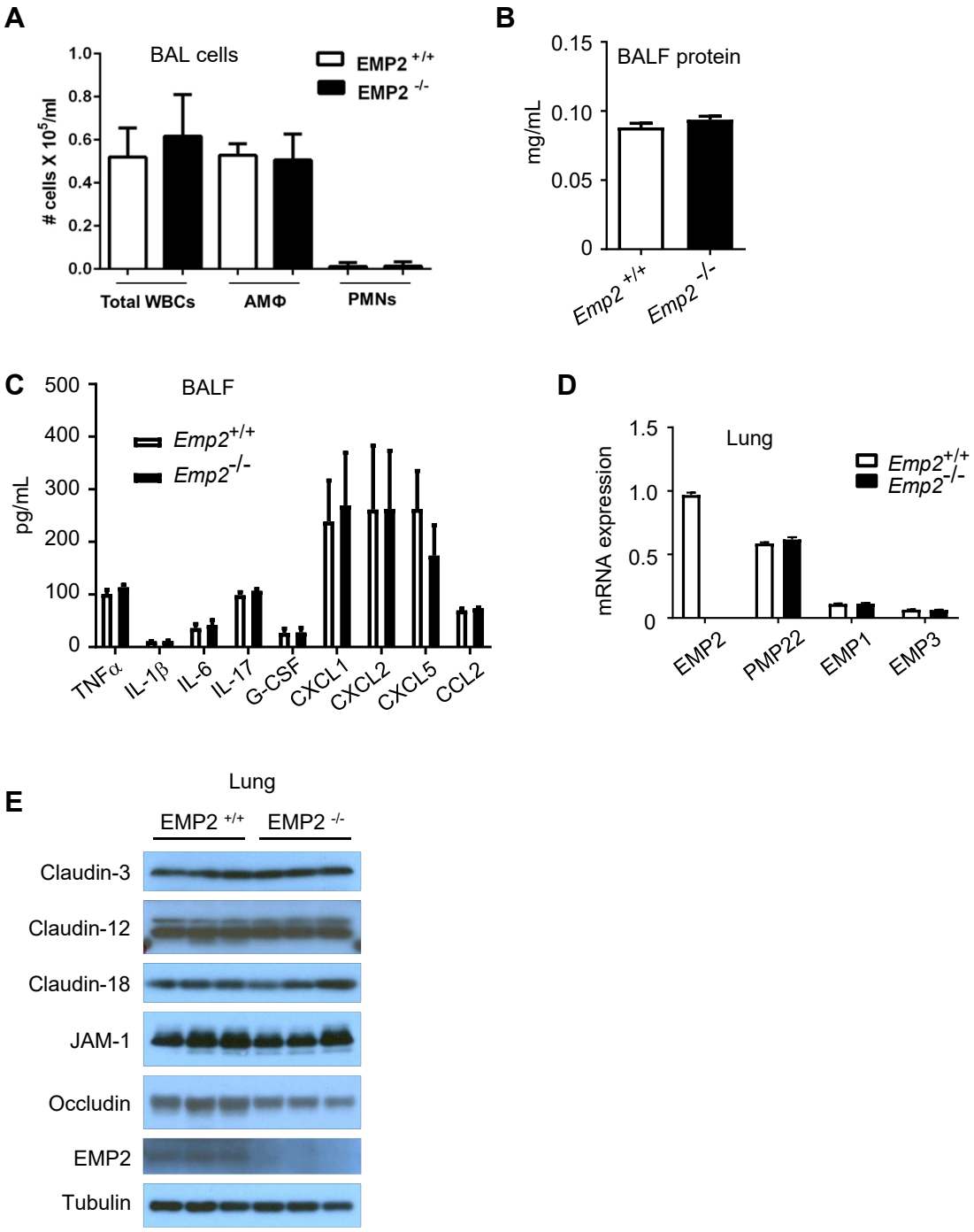

Supplemental Figure 4. Normal basal phenotype of EMP2-null mice. (**A**) Total leukocytes (WBCs), alveolar macrophages (AM), and neutrophils (PMNs) were quantified by morphology in bronchoalveolar lavage (BAL) of naïve *Emp2*$^{+/+}$ and *Emp2*$^{-/-}$ mice (N=5/genotype). (**B**) Protein concentration was quantified in BAL fluid (BALF) (N=5/genotype). (**C**) BALF cytokines and chemokines were quantified (N=5-6/genotype). (**D**) *Emp2, Pmp22, Emp1*, and *Emp3* mRNA were quantified in lung homogenates (N=5/genotype). (**E**) Lung homogenates from naïve *Emp2*$^{+/+}$ and *Emp2*$^{-/-}$ mice (N=3/genotype) were immunoblotted for the targets shown. Graphical data are the mean ± SEM and are representative of at least 2-3 independent experiments.

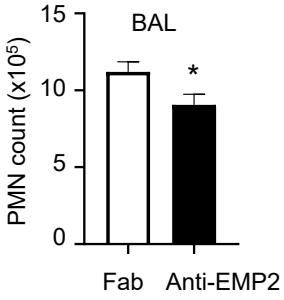

Supplemental Figure 5. EMP2 blockade reduces LPS-induced airspace neutrophilia in wild type mice. C57BL/6 mice were treated i.t. (oropharyngeal aspiration) with 250 μg anti-EMP2 scFv or Fab (control) fragment at -24h and -2h prior to LPS aerosol exposure (300 μg/ml x 30 min). BAL PMNs were quantified at 24h post-LPS (N=15/treatment). Data are the mean ± SEM. *, $P<0.05$ by two-tailed t-test.

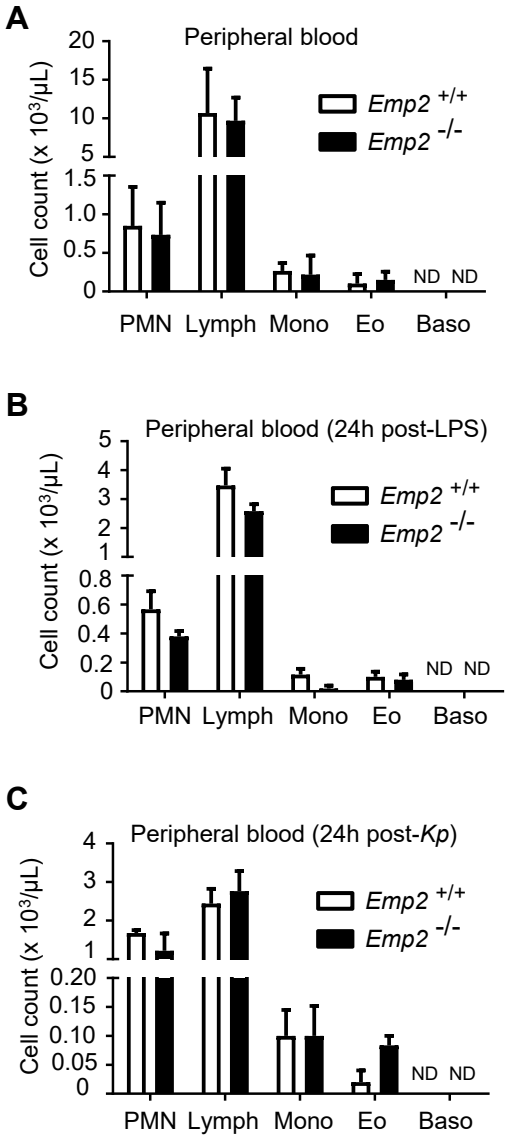

Supplemental Figure 6. Normal circulating leukocyte counts in EMP2-null mice. (**A-C**) Neutrophils (PMNs), lymphocytes (Lymph), monocytes (Mono), eosinophils (Eo), and basophils (Baso) were quantified in peripheral blood of *Emp2*$^{+/+}$ and *Emp2*$^{-/-}$ mice in the naïve state (A), 24h post-LPS inhalation (B), and 24h post-lung infection with *K. pneumoniae* (C) (N=6/genotype). Data are the mean ± SEM and are representative of at least 3 independent experiments. ND=not detected.

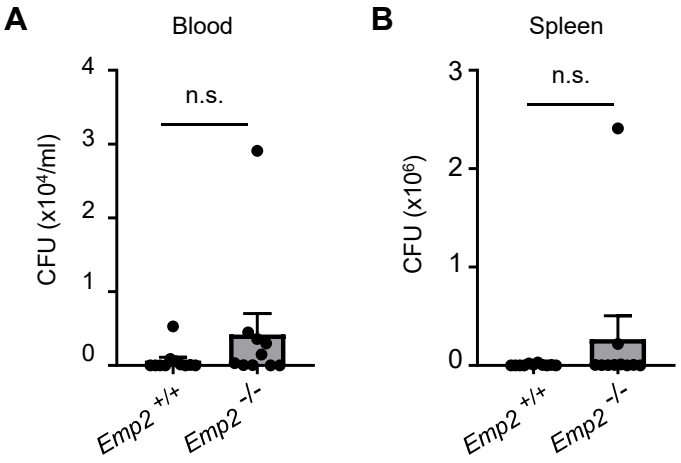

Supplemental Figure 7. Unchanged extrapulmonary bacterial dissemination in EMP2-null mice during pneumonia. (**A-B**) *Emp2*$^{+/+}$ and *Emp2*$^{-/-}$ mice were intratracheally infected with 1000 CFU *K. pneumoniae*. Peripheral blood (A) and splenic homogenate (B) was quantitatively cultured for bacterial burden 72h post-infection. Data shown is representative of two independent experiments (N=9-11 mice/genotype). Not significant (n.s.) by Mann-Whitney test.

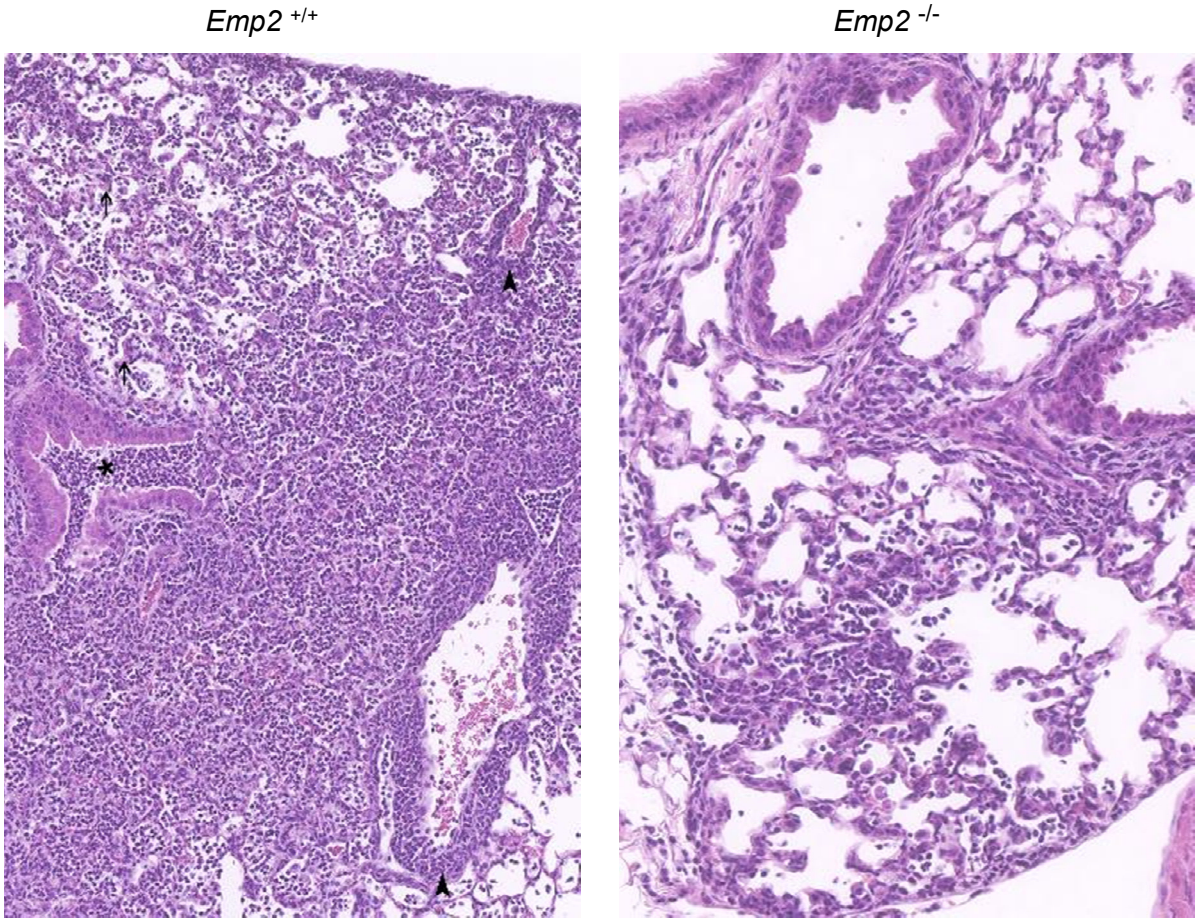

Supplemental Figure 8. Reduced pulmonary histopathology in pneumonic EMP2-null mice. Inflammation in the lungs of *Emp2*$^{+/+}$ mice was more severe than that in *Emp2*$^{-/-}$ counterparts. A representative area of *Emp2*$^{+/+}$ lung shown demonstrates inflammation characterized by thickened alveolar septa (arrows) and infiltration of neutrophils in the alveolar space, bronchioles (asterisk), peribronchiolar areas, and perivascular areas (arrowheads). In comparison, inflammation in *Emp2*$^{-/-}$ mice was minimal. A representative area of *Emp2*$^{-/-}$ lung shown demonstrates inflammation characterized by infiltration of small numbers of macrophages and neutrophils in the alveolar space and thickened alveolar septa. Magnification: *Emp2*$^{+/+}$; 20x; *Emp2*$^{-/-}$; 25x

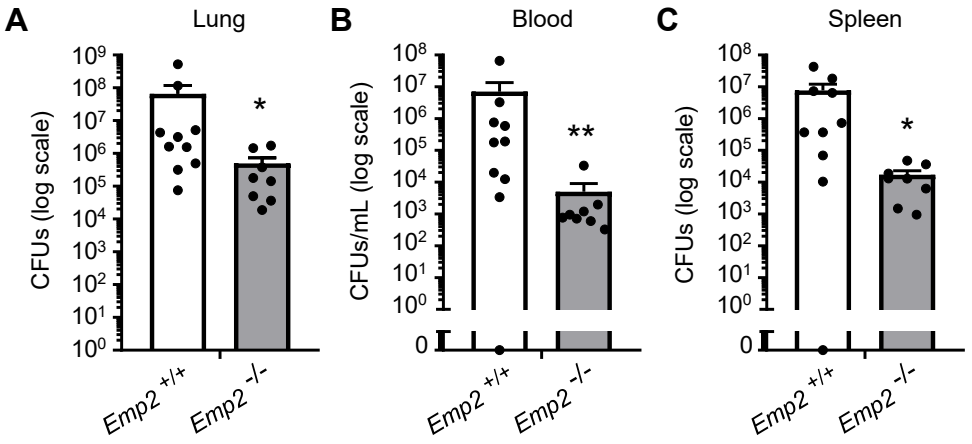

Supplemental Figure 9. Reduced bacterial burden in Emp2-null mice following lung infection. *Emp2*$^{+/+}$ and *Emp2*$^{-/-}$ mice were inoculated in the lungs with 4000 CFU *K. pneumoniae*. At 48h post-infecton, lungs (A), blood (B), and spleen (C) were cultured to determine bacterial burden. N=8-10. *, P<0.05; **, P<0.01 by Mann-Whitney test. In panels B and C, a discontinuous y-axis was used to allow graphical display of zero values.

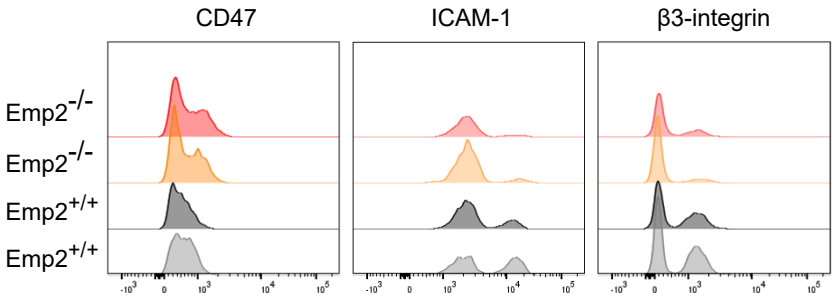

Supplemental Figure 10. Representative flow cytometry histograms. AT1 cells (gating shown in Supplementary Figure 1) from naïve *Emp2*$^{+/+}$ and *Emp2*$^{-/-}$ mice (2 representative mice/genotype are shown) were evaluated by flow cytometry for surface display of CD47, ICAM-1, and β3 integrin.

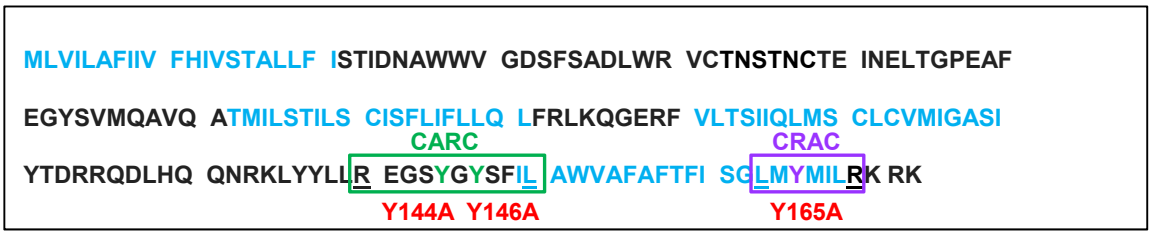

Transmembrane domain
CRAC (Cholesterol recognition/interaction amino acid consensus): (L/V)-X_{1-5} -(Y)-X_{1-5} -(K/R)
CARC or CRAC-like motif (inverted CRAC): (K/R)-X_{1-5} -(Y/F)-X_{1-5} -(L/V)

Supplemental Figure 11. Features of murine EMP2 protein. Mouse EMP2 amino acid sequence is shown. Putative transmembrane domains (blue) are shown as per http://www.uniprot.org/uniprot/Q548I4. Manual inspection of the sequence suggests one putative cholesterol recognition amino acid consensus (CRAC) motif, and two putative reverse CRAC (CARC) sequences. Proposed consensus sequences for CRAC and CARC motifs are shown as reported (Baier CJ et al., *Sci Rep* 2011; Fantini J et al., *Front Physiol* 2013). Tyrosine (Y) residues that were changed to alanine (A) by site-directed mutagenesis in our studies are identified.

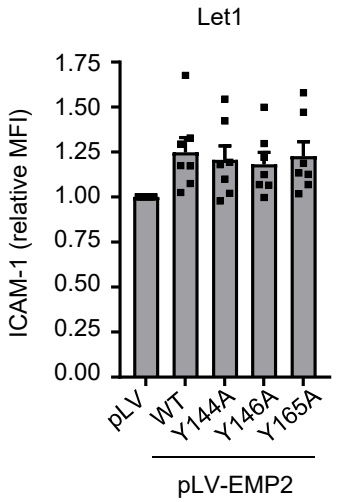

Supplemental Figure 12. Epithelial cells expressing wild type EMP2 and cholesterol-binding motif mutant EMP2 have equivalent ICAM-1 display. Let1 cells transfected with WT EMP2, empty vector (pLV), or EMP2 with site-directed mutagenesis of putative CARC and CRAC cholesterol-binding motifs as in Figure 5 were evaluated by flow cytometry for surface display of ICAM-1. Relative mean fluorescence intensity (MFI) is shown. Data are mean ± SEM and are representative of at least 3 independent experiments.